Physics Letters B 752 (2016) 175–181

Contents lists available at ScienceDirect

Physics Letters B

www.elsevier.com/locate/physletb

Axion cosmology, lattice QCD and the dilute instanton gas

Sz. Borsanyi [a], M. Dierigl [b], Z. Fodor [a,c,d], S.D. Katz [d,e,*], S.W. Mages [f,c], D. Nogradi [d,e,g], J. Redondo [h,i], A. Ringwald [b], K.K. Szabo [a,c]

[a] Department of Physics, Wuppertal University, Gaussstrasse 20, D-42119 Wuppertal, Germany
[b] Deutsches Elektronen-Synchrotron DESY, Notkestrasse 85, D-22607 Hamburg, Germany
[c] IAS/JSC, Forschungszentrum Jülich, D-52425 Jülich, Germany
[d] Institute for Theoretical Physics, Eötvös University, Pázmány Peter sétany 1/A, H-1117 Budapest, Hungary
[e] MTA-ELTE Lendület Lattice Gauge Theory Research Group, Budapest, Hungary
[f] University of Regensburg, D-93053 Regensburg, Germany
[g] Kavli Institute for Theoretical Physics, University of California, Santa Barbara, CA 93106-4030, USA
[h] Departamento de Física Teórica, Universidad de Zaragoza, Pedro Cerbuna 12, E-50009 Zaragoza, Spain
[i] Max-Planck-Institut für Physik (Werner-Heisenberg-Institut), Föhringer Ring 6, D-80805 München, Germany

ARTICLE INFO

Article history:
Received 3 September 2015
Received in revised form 6 November 2015
Accepted 9 November 2015
Available online 11 November 2015
Editor: B. Grinstein

Keywords:
Axion dark matter
QCD on the lattice
Instantons

ABSTRACT

Axions are one of the most attractive dark matter candidates. The evolution of their number density in the early universe can be determined by calculating the topological susceptibility $\chi(T)$ of QCD as a function of the temperature. Lattice QCD provides an *ab initio* technique to carry out such a calculation. A full result needs two ingredients: physical quark masses and a controlled continuum extrapolation from non-vanishing to zero lattice spacings. We determine $\chi(T)$ in the quenched framework (infinitely large quark masses) and extrapolate its values to the continuum limit. The results are compared with the prediction of the dilute instanton gas approximation (DIGA). A nice agreement is found for the temperature dependence, whereas the overall normalization of the DIGA result still differs from the non-perturbative continuum extrapolated lattice results by a factor of order ten. We discuss the consequences of our findings for the prediction of the amount of axion dark matter.

1. Introduction

One of the greatest puzzles in particle physics is the nature of dark matter. A prominent particle candidate for the latter is the axion A [1,2]: a pseudo Nambu–Goldstone boson arising from the breaking of a hypothetical global chiral $U(1)$ extension [3] of the Standard Model at an energy scale f_A much larger than the electroweak scale.

A key input for the prediction of the amount of axion dark matter [4–6] is its potential as a function of the temperature, $V(A,T)$. It is related to the free energy density in QCD, $F(\theta,T) \equiv -\ln Z(\theta,T)/\mathcal{V}$, via

$$V(A,T) \equiv -\frac{1}{\mathcal{V}} \ln \left[\frac{Z(\theta,T)}{Z(0,T)} \right] |_{\theta = A/f_A}, \tag{1}$$

where $\mathcal{V}$ is the Euclidean space–time volume. Here $A(x)$ is the axion field and f_A is the axion decay constant. The axion field has mass dimension one, therefore $A(x)/f_A$ is dimensionless and can be interpreted as an x dependent θ value. The angle θ enters the Euclidean QCD Lagrangian via the additional term involving the topological charge density $q(x)$,

$$-i\theta q(x) \equiv -i\theta \frac{\alpha_s}{16\pi} \epsilon_{\mu\nu\rho\sigma} F^a_{\mu\nu}(x) F^a_{\rho\sigma}(x), \tag{2}$$

with $F^a_{\mu\nu}$ being the gluonic field strength and $\alpha_s \equiv g_s^2/(4\pi)$ the fine structure constant of strong interactions.

On general grounds, the free energy density and thus the axion potential has an absolute minimum at $\theta = A/f_A = 0$. In fact, this is the reason why in this extension of the Standard Model there is no strong CP problem [3]. The curvature around this minimum determines the axion mass m_A at finite temperature,

$$m_A^2(T) \equiv \frac{\partial^2 V(A,T)}{\partial A^2} |_{A=0} = \frac{\chi(T)}{f_A^2}, \tag{3}$$

in terms of the topological susceptibility, i.e. the variance of the $\theta = 0$ topological charge distribution,

* Corresponding author.
E-mail address: katz@bodri.elte.hu (S.D. Katz).

http://dx.doi.org/10.1016/j.physletb.2015.11.020

$$\chi(T) \equiv \int d^4x \langle q(x)q(0)\rangle_T |_{\theta=0} = \lim_{\mathcal{V}\to\infty} \frac{\langle Q^2\rangle_T |_{\theta=0}}{\mathcal{V}}, \tag{4}$$

where $Q \equiv \int d^4x q(x)$. Similarly, self-interaction terms in the potential, e.g. the A^4 term occurring in the expansion of the free energy density around $\theta = A/f_A = 0$,

$$V(A,T) = \frac{1}{2}\chi(T)\theta^2\left[1 + b_2(T)\theta^2 + \ldots\right]|_{\theta=A/f_A}, \tag{5}$$

are determined by higher moments,

$$b_2(T) = -\frac{\langle Q^4\rangle_T - 3\langle Q^2\rangle_T^2}{12\langle Q^2\rangle_T}\,|_{\theta=0}\,. \tag{6}$$

These non-perturbative quantities enter in a prediction of the lower bound on the fractional contribution of axions to the observed cold dark matter as follows[1]

$$R_A \gtrsim 10^5 \langle\theta^2\rangle\, f(\langle\theta^2\rangle) \frac{\mathrm{GeV}^3}{g_{*S}(T_{\rm osc})T_{\rm osc}^3}\sqrt{\frac{\chi(T_{\rm osc})}{\chi(0)}}, \tag{7}$$

where $\langle\theta^2\rangle$ is the variance of the spatial distribution of the initial values of the axion field A/f_A before the formation of the dark matter condensate by the misalignment mechanism, which occurs, when the Hubble expansion rate gets of the order of the axion mass, $m_A(T_{\rm osc}) = 3H(T_{\rm osc})$, i.e. at a temperature

$$T_{\rm osc} \simeq \frac{50\ \mathrm{GeV}}{g_{*R}^{1/4}(T_{\rm osc})}\left(\frac{m_A}{\mu\mathrm{eV}}\right)^{1/2}\left(\frac{\chi(T_{\rm osc})}{\chi(0)}\right)^{1/4}. \tag{8}$$

The function $f(\langle\theta^2\rangle)$ is taking into account anharmonicity effects arising from the self-interaction terms in $V(A,T)$ and depends on the specific form of the potential. The functions $g_{*R}(T)$ and $g_{*S}(T)$ denote the effective number of relativistic energy and entropy degrees of freedom, respectively.

What is urgently needed for axion cosmology is thus a precise determination of the topological susceptibility and higher moments of the topological charge distribution. In this context, most predictions have been entirely based on the semi-classical expansion of the Euclidean path integral of finite temperature QCD around a dilute gas of instantons – finite action minima of the Euclidean action with unit topological charge – see e.g. Ref. [8] for an early exhausting study and Ref. [9] for a recent update concerning the quark masses. A comparative study of these predictions based on the dilute instanton gas approximation (DIGA) has been carried out in Ref. [10], where also an analysis in terms of a phenomenological instanton liquid model (IILM) [11] is presented. However, up to now, in all DIGA investigations of the topological susceptibility only the one-loop expression in the expansion around the instanton background field was used. This results in a strong renormalization scale dependence and thus large uncertainties which were neglected in the previous DIGA based predictions. In fact, in the temperature range $T_{\rm osc} \sim$ GeV of interest, one expects a large uncertainty in the overall normalization due to the neglection of higher order loop effects, since in this region $\alpha_s(T_{\rm osc})$ is not small. We will exploit in this letter both the one-loop DIGA result as well as its two-loop renormalization group improved (RGI) version in order to study the theoretical uncertainties arising from higher loop corrections. Most importantly, we compare these predictions with the outcome of our lattice based fully non-perturbative results.

[1] This is a rewriting of equation (2.10) of Ref. [7] where we have used $\chi(0) = (m_A f_A)^2 \simeq 3.6\times10^{-5}$ GeV^4 from the chiral Lagrangian to express f_A in terms of m_A, the zero temperature mass, that is itself a function of $T_{\rm osc}$ and the ratio $\chi(T)/\chi(0) = (m_A(T)/m_A)^2$ through the condition for the onset of the oscillations, $m_A(T_{\rm osc}) = 3H(T_{\rm osc})$ with $H^2 = 8\pi^3 G_N g_{*R}(T)T^4/90$ the Hubble expansion rate.

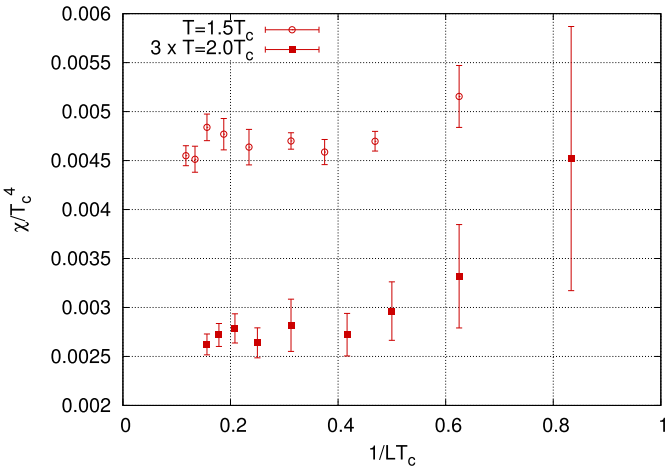

Fig. 1. Demonstration that volume is sufficiently large to have negligible finite volume corrections on Q^2. The data for $T/T_c = 2$ is multiplied by 3 for better visibility of the comparison.

Actually, there have been a number of lattice calculations of $\chi(T)$ and $b_2(T)$ at temperatures below or slightly above the QCD phase transition, mostly in quenched QCD, see e.g. [12–16]. Here we go beyond those lattice calculations. We extend the available temperature range and carry out a controlled continuum extrapolation for this extended range. In addition, note that there has been no quantitative investigation whether and where the lattice results turn into the DIGA results. We will present our new high-quality lattice data for the topological susceptibility in quenched QCD (i.e. neglecting the effects of light quarks) and compare them quantitatively to the DIGA result specialized to the case of $n_f = 0$ light quarks.

2. Axion potential coefficients from the lattice

On the lattice, the topological susceptibility is measured on the torus as the second moment of the distribution of the global topological charge

$$\chi_t = \langle Q^2\rangle/\mathcal{V},$$

where Q is any renormalized discretization of the global topological charge, and $\mathcal{V}$ is the four-volume of the lattice. There are a lot of different fermionic and gluonic definitions of Q available. We choose a gluonic definition based on the Wilson flow [17,18], which has the correct continuum limit similarly to the fermionic definitions but is numerically a lot cheaper. In particular we evolve our gauge field configurations with the Wilson plaquette action to a flow time t and define the global topological charge as the integral over the clover definition of the topological charge density. This definition gives a properly renormalized observable when the flow time t is fixed in physical units.

We use a tree-level Symanzik improved gauge action. Our temperatures range from below T_c up to $4T_c$. Here T_c is the critical temperature, which is the quantity used for scale setting. The critical temperatures for different lattice spacings were determined in earlier work [19,20]. For the whole temperature range we keep the spatial lattice size approximately at $L = 2/T_c$. We checked with dedicated high volume runs at $1.5T_c$ and $2T_c$ that this volume is sufficiently large to have negligible finite volume corrections on Q^2. This is shown in Fig. 1. Our spatial geometry is $L\times L\times 2L$ to enable tests of subvolume methods which will be reported separately – here we only use the full volume. For all temperatures we

Table 1
List of simulation points: temperatures, lattice sizes $N_t = 1/(aT)$, $N_s = L/a$, number of sweeps N_{sweeps}, and estimated integrated autocorrelation time $t_{int,Q}$ are given.

T/T_c	N_t	N_s	N_{sweeps}	$t_{int,Q}$
0.9	12	5	32 K	3.3(2)
	12	6	48 K	7.1(4)
	16	8	170 K	36.4(32)
1.0	12	5	48 K	4.6(2)
	12	6	64 K	12.6(9)
	16	8	180 K	53.9(52)
1.1	12	5	48 K	5.3(3)
	16	6	160 K	12.7(8)
	20	8	330 K	65.3(71)
1.3	16	5	64 K	5.7(3)
	16	6	220 K	15.4(9)
	24	8	550 K	70.2(87)
1.5	16	5	96 K	5.8(2)
	20	6	210 K	14.5(10)
	24	8	660 K	63.8(75)
1.7	20	5	420 K	6.9(2)
	20	6	1300 K	18.9(6)
	28	8	8200 K	88.1(42)
2.0	20	5	440 K	7.5(2)
	24	6	1900 K	18.0(6)
	32	8	8400 K	90.5(51)
2.3	24	5	740 K	8.0(3)
	28	6	2400 K	18.7(5)
	36	8	8500 K	60.4(31)
2.6	28	5	960 K	6.9(2)
	32	6	3500 K	17.8(5)
	44	8	8000 K	51.7(35)
3.0	32	5	1500 K	6.2(2)
	36	6	5700 K	16.0(5)
	48	8	11 000 K	54.3(46)
3.5	36	5	2200 K	5.3(1)
	44	6	5200 K	15.6(6)
	56	8	12 000 K	<45.0
4.0	40	5	2600 K	<5.0
	48	6	5900 K	15.6(8)
	64	8	12 000 K	<45.0

have three lattice spacings $(aT)^{-1} = 5, 6, 8$ to be able to perform an independent continuum extrapolation for every temperature. The local heatbath/overrelaxation algorithm is used for the update, one sweep consists of 1 heatbath and 4 overrelaxation steps. We found that the autocorrelation time of the topological charge depends weakly on (aT), i.e. if the temperature is increased by decreasing the lattice spacing. The number of update sweeps between measurements was chosen in accordance with the autocorrelation time. Table 1 lists the simulation points with the number of sweeps.

We integrated the Wilson flow numerically to a maximum flow-time of about $8t \approx 1/(2T_c^2)$ for all temperatures. Fig. 2 gives the dependence of the susceptibility on the flow time for $T = 2T_c$. While in the continuum limit the result is independent of the choice of the flow time t, different choices have very different lattice artefacts. For small flow times the different lattice spacings give very different results. For larger flow times the expected plateau behavior can be observed for each lattice spacing and the lattice artefacts also decrease significantly. The choice of the flow time brings in some arbitrariness into the analysis, however the continuum result should not depend on this choice once t is fixed in physical units. But this is certainly a subleading source of error compared to the statistical error due to the rare topology tunneling

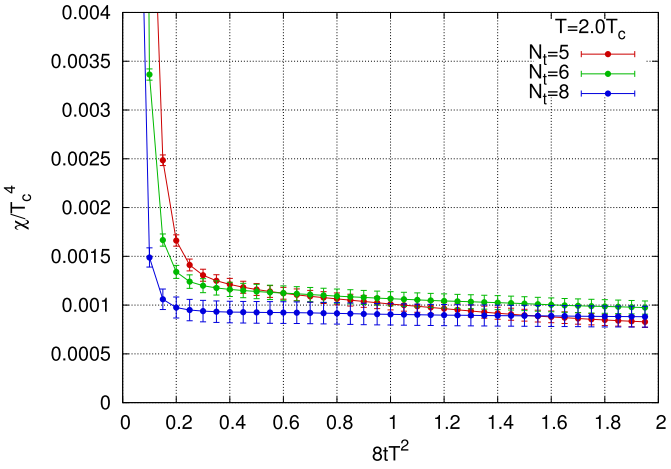

Fig. 2. Demonstration that Wilson flow/lattice renormalization are under control and that the dependence of the results on the choice of the flow time decreases when the continuum limit is approached.

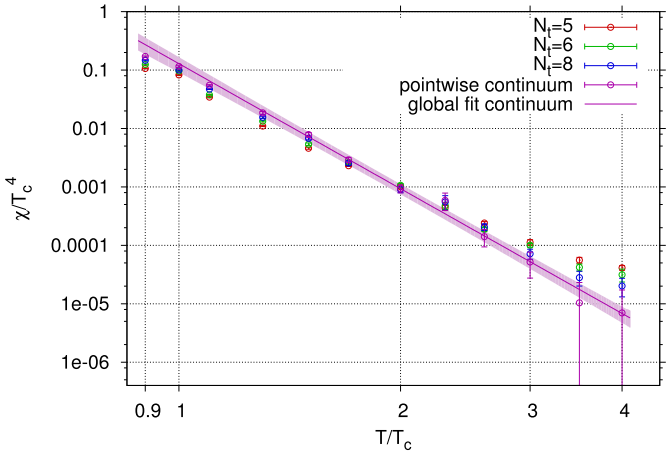

Fig. 3. Lattice data on the topological susceptibility at $N_t = 5, 6, 8$ and lattice continuum extrapolation together with fit of simple power law.

events at high temperatures. In this analysis we choose a temperature dependent flow time for the evaluation of Q^2 as

$$8t = \begin{cases} 1/(1.5T_c)^2, & T < 1.5 \\ 1/T^2, & T \geq 1.5 \end{cases}. \tag{9}$$

For low/high temperatures this means a temperature independent/dependent flow time. This choice is safely in the expected plateau region for all temperatures.

The resulting values for the susceptibility are plotted in Fig. 3. This plot also gives the result of a global continuum extrapolation using a set of temperatures and the 6-parameter power law ansatz

$$\chi_t = (\chi_0 + \chi_0' a^2) \left(\frac{T}{T_0 + T_0' a^2} \right)^{b + b' a^2}, \tag{10}$$

where χ_0, T_0, and b are fit parameters giving the continuum limit. χ_0', T_0', and b' are fit parameters describing the deviation from the continuum limit. The power law form of the fit is motivated by the expected high temperature behavior of the susceptibility. For temperatures close to T_c this is only an empirical fit which seems to describe the lattice results quite well. The fit parameter T_0 is included as a consistency check and should give 1 in units of T_c. This is satisfied by the fit result. The variation between different choices for the starting temperature of the fit range $T_{min}/T_c = 1.3, 1.5, 1.7$

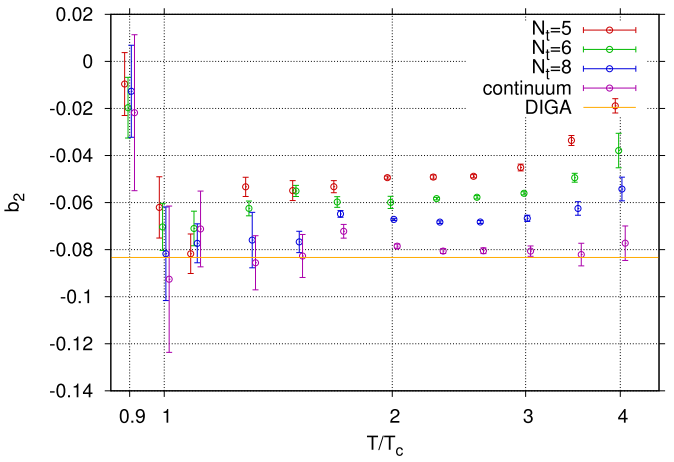

Fig. 4. Lattice data on the anharmonicity coefficient b_2 of the axion potential compared to its DIGA prediction. The data points are shifted a bit horizontally for better visibility.

gives an estimate of the systematic error of the result. The best fit parameters are

$$\chi_0 = 0.11(2)(1), \quad b = -7.1(4)(2), \quad T_0 = 1.02(4)(2), \tag{11}$$

where the first error is the statistical, the second is the systematic. The point-wise continuum extrapolation is consistent with the global fit, evidently the latter has smaller errors for large temperatures. Note that though a controlled continuum extrapolation is possible using three lattice spacings, estimating the systematic uncertainty of this extrapolation would require at least one more lattice resolution.

In a recent analysis [15] the topological susceptibility was calculated using the techniques [21,22]. The calculation was carried out at two temporal extensions, corresponding to two lattice spacings at each temperature. The exponent $b = -5.64(4)$ was found which differs from our value. Note however, that our temperature range is larger, thus we are closer to the applicability range of the DIGA. Furthermore, the two lattice spacings were not sufficient for a controlled continuum extrapolation thus uncertainties related to this final step are not included in the result of [15].

We have also determined the second important coefficient b_2 of the axion potential, characterizing its anharmonicity, by measuring the observable

$$b_{2,t} = -\frac{\langle Q^4\rangle - 3\langle Q^2\rangle^2}{12\langle Q^2\rangle}.$$

The result is plotted in Fig. 4.

3. Comparison between lattice and DIGA results

In this section, we confront the lattice results with the ones obtained from the DIGA framework. For the sake of completeness let us collect first the available formulas for the latter [23–30]. At very high temperatures, far above the QCD phase transition, it makes sense to infer the θ dependence of QCD from the DIGA, in which the partition function, for any n_f, can be written as [24],

$$Z(\theta, T) \simeq \sum_{n_I, n_{\bar I}} \frac{1}{n_I! n_{\bar I}!} Z_I^{n_I+n_{\bar I}}(T) \exp\left[i\theta(n_I - n_{\bar I})\right], \tag{12}$$

where $Z_I = Z_{\bar I}$ is the contribution arising from the expansion of the path integral around a single instanton I (anti-instanton $\bar I$). It follows directly that the potential has the form

$$V(A, T) \simeq \chi(T)\,(1 - \cos\theta)\,|_{\theta = A/f_A}, \tag{13}$$

from which one infers

$$b_2(T) \simeq -\frac{1}{12}. \tag{14}$$

This can be confronted right-away with our lattice results, cf. Fig. 4. Similar to Ref. [13] we find that the prediction from the DIGA for b_2 is reached already at surprisingly low values of $T/T_c \gtrsim 1$.

The whole temperature dependence of the axion potential arises in the DIGA through the topological susceptibility, which in this case is explicitly given by

$$\chi(T) \simeq \frac{Z_I(T) + Z_{\bar I}(T)}{\mathcal{V}} = 2\int_0^\infty d\rho\, D(\rho)\, G(\pi\rho T), \tag{15}$$

in terms of the instanton size distribution at zero temperature, $D(\rho)$, and a factor $G(\pi\rho T)$ taking into account finite temperature effects. The former is known in the framework of the semiclassical expansion around the instanton for small $\alpha_s(\mu_r)\ln(\rho\,\mu_r)$ and $\rho\, m_i(\mu_r)$, where α_s is the strong coupling, μ_r is the renormalization scale and $m_i(\mu_r)$ are the running quark masses. To one-loop accuracy, it is given by[2]

$$D(\rho) \equiv \frac{d_{\overline{\rm MS}}}{\rho^5}\left(\frac{2\pi}{\alpha_{\overline{\rm MS}}(\mu_r)}\right)^6 \exp\left(-\frac{2\pi}{\alpha_{\overline{\rm MS}}(\mu_r)}\right) \times (\rho\,\mu_r)^{\beta_0}\left[1 + \mathcal{O}(\alpha_{\overline{\rm MS}}(\mu_r))\right], \tag{16}$$

with

$$d_{\overline{\rm MS}} = \frac{e^{5/6}}{\pi^2}\, e^{-4.534122}; \quad \beta_0 = 11. \tag{17}$$

At finite temperature, electric Debye screening prohibits the existence of large-scale coherent fields in the plasma, leading to the factor [26,27],

$$G(x) \equiv \exp\left\{-2x^2 - 18A(x)\right\}, \tag{18}$$

with

$$A(x) \simeq -\frac{1}{12}\ln\left[1 + (\pi\rho T)^2/3\right] + \alpha\left[1 + \gamma(\pi\rho T)^{-3/2}\right]^{-8}, \tag{19}$$

and $\alpha = 0.01289764$ and $\gamma = 0.15858$, in Eq. (15). This factor cuts off the integration over the size distribution in Eq. (15) at $x = \pi\rho T \sim 1$ and ensures the validity of the DIGA at large temperatures, at which $\alpha_s(\pi T) \ll 1$.

Collecting all the factors, the topological susceptibility, in the one-loop DIGA, reads

$$\chi(T) \simeq 2\, d_{\overline{\rm MS}}\,(\pi T)^4 \left(\frac{\mu_r}{\pi T}\right)^{11} I \left(\frac{2\pi}{\alpha_{\overline{\rm MS}}(\mu_r)}\right)^6 \times \exp\left(-\frac{2\pi}{\alpha_{\overline{\rm MS}}(\mu_r)}\right)\left[1 + \mathcal{O}(\alpha_{\overline{\rm MS}}(\mu_r))\right], \tag{20}$$

with

$$I = \int_0^\infty dx\, x^6\, G(x) = 0.267271. \tag{21}$$

This result, however, still suffers from a sizeable dependence on the renormalization scale μ_r, reflecting the importance of the neglected two-loop and higher order contributions. In fact, it is

[2] For quenched QCD the number of light quarks is $n_f = 0$; the general formula can be found explicitly in e.g. Ref. [30], which contains a pioneering confrontation of cooled lattice data on $D(\rho)$ with the two-loop RG improved DIGA result.

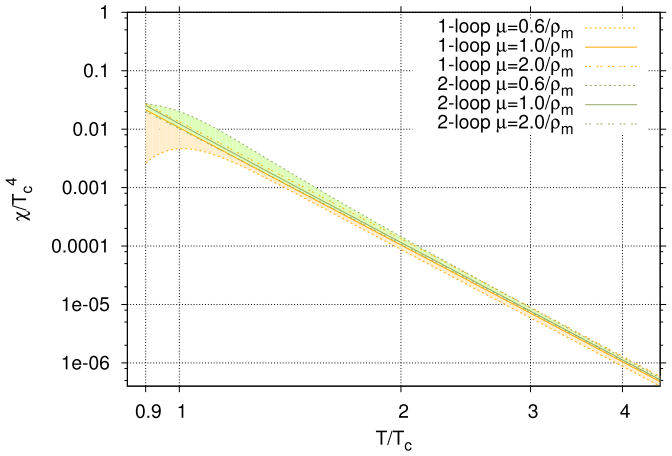

Fig. 5. Prediction of the topological susceptibility in the DIGA: comparison between one-loop and two-loop RGI results. We used the four-loop expression for the running coupling in the modified minimal subtraction scheme as given in the appendix of Ref. [31] and the central value of $T_c/\Lambda_{\overline{\rm MS}}^{(n_f=0)} = 1.26(7)$ as determined from the lattice in Ref. [20].

Table 2
Temperature slopes of the topological susceptibility predicted in the two-loop RGI DIGA, for a range of renormalization scales according to Eq. (24).

T/T_c	1.5	2	3	4	5
b ($\kappa = 0.6$)	−6.04	−6.26	−6.43	−6.50	−6.55
b ($\kappa = 1$)	−6.37	−6.46	−6.55	−6.59	−6.62
b ($\kappa = 2$)	−6.55	−6.59	−6.64	−6.67	−6.69

tamed by taking into account the ultraviolet part of the two-loop correction. The latter has been calculated in Ref. [29] and shown to have exactly the form that the gauge coupling becomes a parameter running according to the renormalization group (RG). Therefore, the ultimate, all order result for the topological susceptibility becomes independent of μ_r, for $\mu_r \to \infty$. At two loop, the corrections amount to a factor

$$(\rho\mu_r)^{(\beta_1 - 12\,\beta_0)\,\alpha_{\overline{\rm MS}}(\mu_r)/(4\pi)}; \quad \beta_1 = 102, \tag{22}$$

in $D(\rho)$. Therefore, this RG improvement can be taken into account by replacing the factor I in Eq. (20) by

$$\tilde{I} = \left(\frac{\mu_r}{\pi T}\right)^{-30\,\alpha_{\overline{\rm MS}}(\mu_r)/(4\pi)} \int_0^\infty dx\, x^{6-30\,\alpha_{\overline{\rm MS}}(\mu_r)/(4\pi)}\, G(x). \tag{23}$$

In fact, exploiting the two-loop RG improvement, the μ_r dependence is heavily reduced, as is obvious from Fig. 5, where we have used as a natural renormalization scale

$$\mu_r = \kappa/\rho_m = \kappa\pi T/1.2, \tag{24}$$

with ρ_m being approximately the maximum of the integrand of $\tilde{I}$, and varied the remaining free parameter κ between 0.6 and 2. The renormalization scale dependence appears to be highly reduced in the regimes $> 3T_c$ and $< T_c$. However, in an intermediate region, $\sim T_c$–$2T_c$, it is comparable in size to the one at one-loop.

We present in Table 2 the power-law behavior predicted by the two-loop RGI DIGA at various temperatures, which can be compared to the fit (11) to the continuum lattice result. As far as the overall normalization of the DIGA result for χ is concerned, one still expects a large uncertainty in the temperature range available from the lattice. In fact, at these temperatures, α_s is not small, see Table 3. Apart from the ultraviolet part, there will be a finite part of the two-loop correction which will affect mainly the overall normalization of χ and will depend on the temperature only

Table 3
Strong coupling constant at $\mu_r = 1/\rho_m$ for the temperature range covered by the lattice.

T/T_c	1	2	3	4	5
$\alpha_{\overline{\rm MS}}(1/\rho_m)$	0.36	0.23	0.19	0.17	0.16

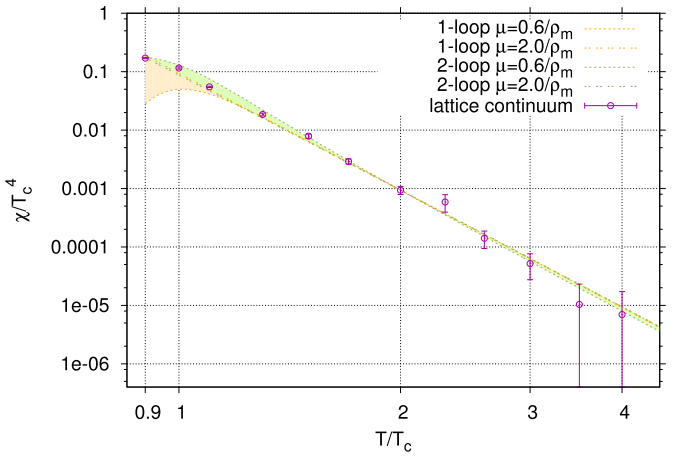

Fig. 6. Rescaled one-loop and two-loop RGI DIGA results compared to lattice continuum extrapolation. The DIGA results shown in Fig. 5 were scaled by a factor K of order ten such that they coincide at $T/T_c = 2$ with the central value of the lattice continuum data.

logarithmically. Unfortunately, this finite part is not known, yet. Therefore, when comparing to the continuum extrapolated lattice results, we allow a multiplicative factor K to account for this uncertainty, i.e. we absorb the remaining higher loop uncertainties by replacing

$$\left[1 + \mathcal{O}(\alpha_{\overline{\rm MS}}(\mu_r = \kappa\pi T/1.2))\right] \to K(T/T_c) \tag{25}$$

in Eq. (20) and the corresponding two-loop RGI expression. Clearly, the K-factor should approach unity at very large T/T_c.

Fig. 6 nicely illustrates the agreement between the DIGA and the lattice result, if a K-factor of order ten is included.[3] More precisely, fitting the lattice continuum data with the rescaled DIGA expression in the temperature range $T/T_c \geq 1$, one finds

$$K = 8.9 \pm 0.7\,, \quad \text{at } 95\%\,\text{CL}, \tag{26}$$

while a fit in the temperature range $T/T_c \geq 2$ yields

$$K = 7.9 \pm 3.3\,, \quad \text{at } 95\%\,\text{CL}. \tag{27}$$

Apparently, in the temperature range accessible to the lattice, the higher order corrections to the pre-factor of the DIGA are still appreciable, but there are indications of a trend that the K-factor gets smaller, as expected, towards larger values of T/T_c.

The K-factor strongly depends on the value of $T_c//\Lambda_{\overline{\rm MS}}^{(n_f=0)}$: it reduces to one for $T_c//\Lambda_{\overline{\rm MS}}^{(n_f=0)} \simeq 1.03$. However, the latter value is about 3 sigma below the central value determined in Ref. [20], $T_c//\Lambda_{\overline{\rm MS}}^{(n_f=0)} \simeq 1.26(7)$.

4. Conclusions

This paper presents lattice and DIGA calculations of the θ and temperature dependence of the free energy density of QCD in the

[3] K factors of order ten to fifty are not uncommon even at next-to-leading order in ordinary perturbative QCD, see e.g. Ref. [32].

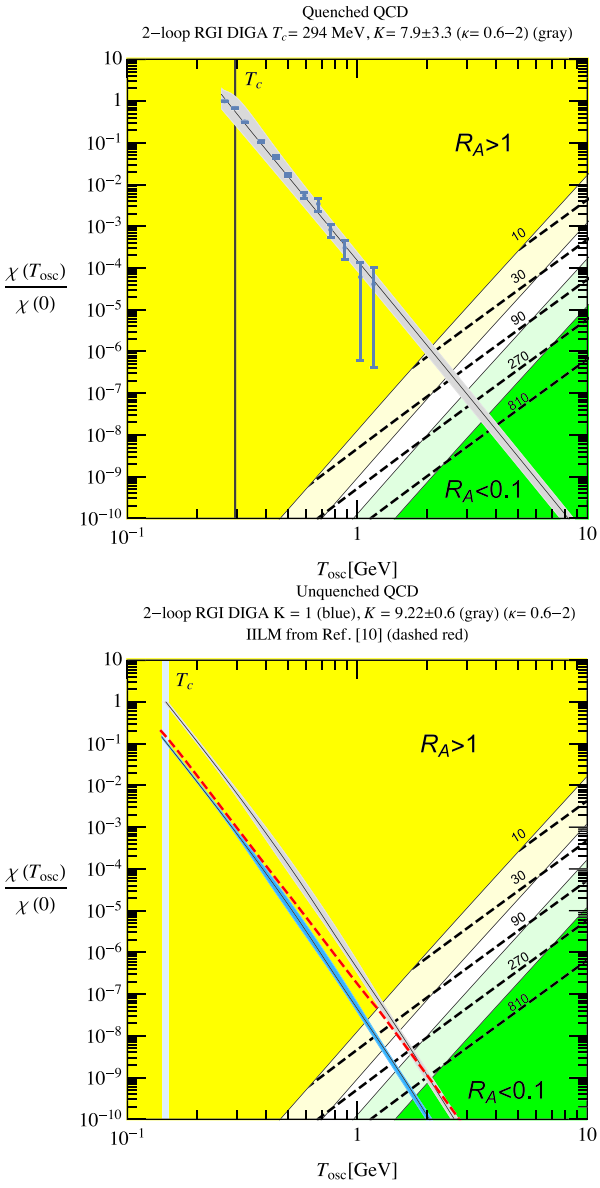

Fig. 7. Consequence of our findings for axion dark matter from quenched (top) and full QCD (bottom). The dark yellow region is excluded because $R_A > 1$ just from the misalignment mechanism, cf. Eq. (7), assuming a flat distribution of initial misalignment angles in the observable universe $\theta \in [-\pi, \pi]$. The light yellow region indicates $R_A > 1$ when string contributions according to Ref. [33] are included. In the dark green region axions even including strings give a small contribution ($R_A < 0.1$) to dark matter. The light green region indicates $R_A < 0.1$ just from the misalignment mechanism. In order to compare the quenched results with the axion dark matter scenario we had to transform dimensionless quantities into dimensionful ones. For illustrative purposes we use, in the quenched case, $T_c = 294$ MeV. Our quenched lattice results are shown by the blue points and the two-loop RGI DIGA prediction by the gray band in the top panel. Since the transition in full QCD is a crossover [34], T_c is not unambiguous even in the unquenched case. Using the transition temperature defined by the chiral susceptibility, $T_c = 147(2)(3)$ MeV [35–37], we need $K = 9.22 \pm 0.6$ in order that the two-loop RGI DIGA matches $\chi(T_c)/\chi(0) = 1$. The blue and gray bands in the lower panel correspond to the two-loop RGI DIGA predictions with $K = 1$ and $K = 9.22 \pm 0.6$, respectively. The dashed red line shows the IILM prediction of Ref. [11]. The dashed black lines correspond to fixed axion masses (in units of μeV). Using $K = 9.22$ and again assuming at least ten percent axion contribution to dark matter we can read off from the lower panel the range 40 μeV $\lesssim m_A \lesssim$ 930 μeV, while using $K = 1$ we would get 50 μeV $\lesssim m_A \lesssim$ 1100 μeV, i.e. only a ∼20% correction for an $\mathcal{O}(10)$ K factor uncertainty. (For interpretation of the references to color in this figure legend, the reader is referred to the web version of this article.)

quenched limit, i.e. for infinite quark masses. In the lattice approach the temperature ranges from $0.9T_c$ to $4T_c$ and thus significantly extends former results. The comparison of the quenched continuum extrapolated lattice data and the DIGA framework has led to two highly non-trivial findings. The first one is the observation that the exponent of the temperature dependence of $\chi(T)$ is correctly described by the DIGA, even all the way down to T_c (at least within our error bars), cf. Fig. 7 (top). The second non-trivial finding is about the prefactor of this temperature dependence: the one-loop based DIGA prefactor is off by a large factor of about ten (we call this a K-factor, a familiar notion in perturbative QCD predictions). This is expected, since in the considered temperature range the strong coupling is still sizeable. However, such a K-factor uncertainty has not been accounted for in any of the previous studies of the axion dark matter abundance, e.g. Refs. [8,9]. Nevertheless, there is a piece of physics information, which essentially fixes this K-factor. As expected, the topological susceptibility changes only a little from $T = 0$ to $T = T_c$ and drops further on for $T > T_c$. Actually, the quenched data is very well described if one takes $\chi(T)/\chi(0) = 1$ at $T/T_c \sim 1$ in order to fix the K-factor[4] and then uses the exponent of the DIGA framework for the rest of the temperature dependence in the high temperature plasma phase, cf. Fig. 7 (top).

Unquenched lattice simulations with physical quark masses are about two-to-three orders of magnitude more CPU intensive than quenched ones. In addition one expects much smaller topological susceptibilities and larger cutoff effects. If one combines all these cost factors one ends up with a very CPU demanding project. Thus, it is of extreme importance to give an estimate of the ranges in temperature and topological susceptibility of interest for axion cosmology.

This can be done by exploiting the two highly non-trivial observations we discussed above: we set $\chi(T_c)/\chi(0) = 1$ and use the exponent suggested by the DIGA framework, which is readily available also for full QCD, for the temperature dependence.[5] Our finding is shown in the lower panel of Fig. 7, where also the result with the DIGA prefactor and that of the interacting instanton liquid model are depicted. Fortunately, the estimated value of the K-factor does not affect very strongly the extraction of the values of the axion mass of interest for axion dark matter, because of the steepness of the falloff of $\chi(T)$, cf. Fig. 7 (bottom).

There are two important messages, which dominantly influence any future lattice study. The first one is that one needs somewhat larger T/T_c values than in the quenched case making the calculation quite CPU demanding. The other important message is that using dynamical QCD one has to determine about one order of magnitude smaller values of $\chi(T)/\chi(0)$ than in the quenched case. Since already $\chi(0)$ is far less in the unquenched case than in the quenched one, the smallness of the needed $\chi(T)/\chi(0)$ makes the task even more CPU demanding. The planning of any future unquenched project should consider the estimates listed above.

Acknowledgements

The authors wish to thank G. Moore for useful discussions. Computations were performed on JUQUEEN at FZ-Jülich and on GPU clusters at Wuppertal and Budapest. This project was funded by the DFG grant SFB/TR55. by OTKA under grant OTKA-NF-104034

[4] We obtain $K = 11.7^{+5.5}_{-3.1}$ by taking $\chi(T_c)/\chi(0) = 1$, where the errors come from varying κ in the (0.5,2) interval, and $K = 7.9 \pm 3.3$, by taking $\chi(T)/\chi(0) = 1$ at $T/T_c = 0.92$, for $\kappa = 1$.

[5] Qualitatively, both the approximate constancy of $\chi(T)/\chi(0)$ for $T/T_c \lesssim 1$ as well as the rapid fall off for $T/T_c \gtrsim 1$ have been observed already in pioneering lattice studies in full QCD [12,14].

and by the National Science Foundation under Grant No. NSF PHY11-25915. S.D.K. is funded by the "Lendület" program of the Hungarian Academy of Sciences (LP2012-44/2012). M.D. acknowledges support from the Studienstiftung des Deutschen Volkes and J.R. from the Ramon y Cajal Fellowship 2012-10597 from the Spanish Ministry of Economy and Competitivity.

References

[1] S. Weinberg, A new light boson? Phys. Rev. Lett. 40 (1978) 223–226, http://dx.doi.org/10.1103/PhysRevLett.40.223.
[2] F. Wilczek, Problem of strong P and T invariance in the presence of instantons, Phys. Rev. Lett. 40 (1978) 279–282, http://dx.doi.org/10.1103/PhysRevLett.40.279.
[3] R.D. Peccei, H.R. Quinn, CP conservation in the presence of instantons, Phys. Rev. Lett. 38 (1977) 1440–1443, http://dx.doi.org/10.1103/PhysRevLett.38.1440.
[4] J. Preskill, M.B. Wise, F. Wilczek, Cosmology of the invisible axion, Phys. Lett. B 120 (1983) 127–132, http://dx.doi.org/10.1016/0370-2693(83)90637-8.
[5] L.F. Abbott, P. Sikivie, A cosmological bound on the invisible axion, Phys. Lett. B 120 (1983) 133–136, http://dx.doi.org/10.1016/0370-2693(83)90638-X.
[6] M. Dine, W. Fischler, The not so harmless axion, Phys. Lett. B 120 (1983) 137–141, http://dx.doi.org/10.1016/0370-2693(83)90639-1.
[7] P. Arias, D. Cadamuro, M. Goodsell, J. Jaeckel, J. Redondo, A. Ringwald, WISPy cold dark matter, J. Cosmol. Astropart. Phys. 1206 (2012) 013, http://dx.doi.org/10.1088/1475-7516/2012/06/013, arXiv:1201.5902.
[8] M.S. Turner, Cosmic and local mass density of invisible axions, Phys. Rev. D 33 (1986) 889–896, http://dx.doi.org/10.1103/PhysRevD.33.889.
[9] K.J. Bae, J.-H. Huh, J.E. Kim, Update of axion CDM energy, J. Cosmol. Astropart. Phys. 0809 (2008) 005, http://dx.doi.org/10.1088/1475-7516/2008/09/005, arXiv:0806.0497.
[10] O. Wantz, E.P.S. Shellard, Axion cosmology revisited, Phys. Rev. D 82 (2010) 123508, http://dx.doi.org/10.1103/PhysRevD.82.123508, arXiv:0910.1066.
[11] O. Wantz, E.P.S. Shellard, The topological susceptibility from grand canonical simulations in the interacting instanton liquid model: chiral phase transition and axion mass, Nucl. Phys. B 829 (2010) 110–160, http://dx.doi.org/10.1016/j.nuclphysb.2009.12.005, arXiv:0908.0324.
[12] B. Alles, M. D'Elia, A. Di Giacomo, Topological susceptibility in full QCD at zero and finite temperature, Phys. Lett. B 483 (2000) 139–143, http://dx.doi.org/10.1016/S0370-2693(00)00556-6, arXiv:hep-lat/0004020.
[13] C. Bonati, M. D'Elia, H. Panagopoulos, E. Vicari, Change of θ dependence in 4D SU(N) gauge theories across the deconfinement transition, Phys. Rev. Lett. 110 (25) (2013) 252003, http://dx.doi.org/10.1103/PhysRevLett.110.252003, arXiv:1301.7640.
[14] V.G. Bornyakov, E.M. Ilgenfritz, B.V. Martemyanov, V.K. Mitrjushkin, M. Müller-Preussker, Topology across the finite temperature transition studied by overimproved cooling in gluodynamics and QCD, Phys. Rev. D 87 (11) (2013) 114508, http://dx.doi.org/10.1103/PhysRevD.87.114508, arXiv:1304.0935.
[15] E. Berkowitz, M.I. Buchoff, E. Rinaldi, Lattice QCD input for axion cosmology, Phys. Rev. D 92 (3) (2015) 034507, http://dx.doi.org/10.1103/PhysRevD.92.034507, arXiv:1505.07455.
[16] R. Kitano, N. Yamada, Topology in QCD and the axion abundance, arXiv:1506.00370.
[17] M. Luscher, Properties and uses of the Wilson flow in lattice QCD, J. High Energy Phys. 08 (2010) 071, http://dx.doi.org/10.1007/JHEP08(2010)071, arXiv:1006.4518;
M. Luscher, J. High Energy Phys. 03 (2014) 092, http://dx.doi.org/10.1007/JHEP03(2014)092, Erratum.
[18] M. Luscher, P. Weisz, Perturbative analysis of the gradient flow in non-abelian gauge theories, J. High Energy Phys. 02 (2011) 051, http://dx.doi.org/10.1007/JHEP02(2011)051, arXiv:1101.0963.
[19] G. Cella, G. Curci, A. Vicere, B. Vigna, The SU(3) deconfining phase transition with Symanzik action, Phys. Lett. B 333 (1994) 457–460, http://dx.doi.org/10.1016/0370-2693(94)90167-8, arXiv:hep-lat/9405018.
[20] S. Borsanyi, G. Endrodi, Z. Fodor, S.D. Katz, K.K. Szabo, Precision SU(3) lattice thermodynamics for a large temperature range, J. High Energy Phys. 07 (2012) 056, http://dx.doi.org/10.1007/JHEP07(2012)056, arXiv:1204.6184.
[21] L. Del Debbio, H. Panagopoulos, E. Vicari, theta dependence of SU(N) gauge theories, J. High Energy Phys. 08 (2002) 044, http://dx.doi.org/10.1088/1126-6708/2002/08/044, arXiv:hep-th/0204125.
[22] S. Durr, Z. Fodor, C. Hoelbling, T. Kurth, Precision study of the SU(3) topological susceptibility in the continuum, J. High Energy Phys. 04 (2007) 055, http://dx.doi.org/10.1088/1126-6708/2007/04/055, arXiv:hep-lat/0612021.
[23] G. 't Hooft, Computation of the quantum effects due to a four-dimensional pseudoparticle, Phys. Rev. D 14 (1976) 3432–3450, http://dx.doi.org/10.1103/PhysRevD.18.2199.3;
G. 't Hooft, Phys. Rev. D 18 (1978) 2199, http://dx.doi.org/10.1103/PhysRevD.14.3432, Erratum.
[24] C.G. Callan Jr., R.F. Dashen, D.J. Gross, Toward a theory of the strong interactions, Phys. Rev. D 17 (1978) 2717, http://dx.doi.org/10.1103/PhysRevD.17.2717.
[25] C.W. Bernard, Gauge zero modes, instanton determinants, and QCD calculations, Phys. Rev. D 19 (1979) 3013, http://dx.doi.org/10.1103/PhysRevD.19.3013.
[26] R.D. Pisarski, L.G. Yaffe, The density of instantons at finite temperature, Phys. Lett. B 97 (1980) 110–112, http://dx.doi.org/10.1016/0370-2693(80)90559-6.
[27] D.J. Gross, R.D. Pisarski, L.G. Yaffe, QCD and instantons at finite temperature, Rev. Mod. Phys. 53 (1981) 43, http://dx.doi.org/10.1103/RevModPhys.53.43.
[28] M. Luscher, A semiclassical formula for the topological susceptibility in a finite space–time volume, Nucl. Phys. B 205 (1982) 483, http://dx.doi.org/10.1016/0550-3213(82)90371-6.
[29] T.R. Morris, D.A. Ross, C.T. Sachrajda, Higher order quantum corrections in the presence of an instanton background field, Nucl. Phys. B 255 (1985) 115, http://dx.doi.org/10.1016/0550-3213(85)90131-2.
[30] A. Ringwald, F. Schrempp, Confronting instanton perturbation theory with QCD lattice results, Phys. Lett. B 459 (1999) 249–258, http://dx.doi.org/10.1016/S0370-2693(99)00682-6, arXiv:hep-lat/9903039.
[31] K.G. Chetyrkin, B.A. Kniehl, M. Steinhauser, Decoupling relations to O (alpha-s**3) and their connection to low-energy theorems, Nucl. Phys. B 510 (1998) 61–87, http://dx.doi.org/10.1016/S0550-3213(97)00649-4, arXiv:hep-ph/9708255.
[32] M. Rubin, G.P. Salam, S. Sapeta, Giant QCD K-factors beyond NLO, J. High Energy Phys. 09 (2010) 084, http://dx.doi.org/10.1007/JHEP09(2010)084, arXiv:1006.2144.
[33] M. Kawasaki, K. Saikawa, T. Sekiguchi, Axion dark matter from topological defects, Phys. Rev. D 91 (6) (2015) 065014, http://dx.doi.org/10.1103/PhysRevD.91.065014, arXiv:1412.0789.
[34] Y. Aoki, G. Endrodi, Z. Fodor, S.D. Katz, K.K. Szabo, The order of the quantum chromodynamics transition predicted by the standard model of particle physics, Nature 443 (2006) 675–678, http://dx.doi.org/10.1038/nature05120, arXiv:hep-lat/0611014.
[35] Y. Aoki, Z. Fodor, S.D. Katz, K.K. Szabo, The QCD transition temperature: results with physical masses in the continuum limit, Phys. Lett. B 643 (2006) 46–54, http://dx.doi.org/10.1016/j.physletb.2006.10.021, arXiv:hep-lat/0609068.
[36] Y. Aoki, S. Borsanyi, S. Durr, Z. Fodor, S.D. Katz, S. Krieg, K.K. Szabo, The QCD transition temperature: results with physical masses in the continuum limit II, J. High Energy Phys. 06 (2009) 088, http://dx.doi.org/10.1088/1126-6708/2009/06/088, arXiv:0903.4155.
[37] S. Borsanyi, Z. Fodor, C. Hoelbling, S.D. Katz, S. Krieg, C. Ratti, K.K. Szabo, Is there still any Tc mystery in lattice QCD? Results with physical masses in the continuum limit III, J. High Energy Phys. 09 (2010) 073, http://dx.doi.org/10.1007/JHEP09(2010)073, arXiv:1005.3508.